2. K. Caldeira, M. R. Rampino, T. Volk, J. C. Zachos, in *Extinction Events in Earth History*, E. G. Kaufman and O. H. Walliser, Eds. (Springer-Verlag, Berlin, 1990), pp. 333–345.
3. E. Baker and E. H. Morgan, in *Iron Metabolism in Health and Disease*, J. H. Brock, J. W. Halliday, M. J. Pippard, L. W. Powell, Eds. (Saunders, Philadelphia, PA, 1994), pp. 63–96.
4. T. D. Bullen and P. M. McMahon, *Min. Mag.* **62A**, 255 (1998).
5. C. N. Marechal, P. Telouk, F. Albarede, *Chem. Geol.* **156**, 251 (1999).
6. P. R. Dixon *et al.*, in *Water Rock Interaction*, vol. 2, *Moderate and High Temperature Environments*, Y. K. Kharaka and A. S. Maest, Eds. (Balkema. Rotterdam, Netherlands, 1992), pp. 915–918.
7. B. L. Beard and C. M. Johnson, *Geochim. Cosmochim. Acta*, in press.
8. C. M. Johnson and B. L. Beard, *Int. J. Mass Spectrom. Ion Proc.* **63**, 1653 (1999).
9. A mixed double spike composed of 7.8% ^{58}Fe and 92.2% ^{54}Fe was added to an aliquot of each analyzed sample to normalize the measured iron isotope ratios for instrumental mass bias.
10. U.W.-Milwaukee experiments were performed in a Coy Laboratory anaerobic hood; ferrihydrite was produced according to the method of C.-F. Lin and M. Benjamin [*Environ. Sci. Technol.* **24**, 126 (1990)]; LM growth medium is 0.1 g of peptone, 0.2 g of yeast extract, and 1 g of NaCl per liter of H_2O [C. R. Myers and J. M. Myers, *J. Appl. Bacteriol.* **76**, 253 (1993); B. Little *et al.*, in *CORROSION/97* (Paper No. 215, NACE International, Houston, TX, 1997). Each experiment was run with 2×10^7 cells/ml.
11. LB growth medium is 10 g of tryptone, 5 g of yeast extract and 1 g of NaCl per liter of H_2O. Ferrihydrite was made according to the method of U. Schwertmann and R. M. Cornell [*Iron Oxides in the Laboratory: Preparation and Characterization* (V.C.H., New York, 1991)]. Each experiment was run in 1-liter polycarbonate bottles filled with the LB growth media, 0.5 g of ferrihydrite, and 5×10^6 cells/ml.
12. Fe(II) contents were determined with the ferrozine technique [L. C. Stookey, *Anal. Chem.* **42**, 779 (1970)]. Ferrozine (1 g/liter) in Hepes buffer (50 mM) at pH 7 was used. A 0.1-ml sample, filtered through a 0.2-μm syringe filter, was mixed with 5 ml of the ferrozine solution. After about 5 min, the absorbance was measured at 562 nm on a spectrophotometer, which had been calibrated with Fe(II) solutions.
13. T. D. Bullen and P. M. McMahon, *Eos* **78**, S173 (1997).
14. K. H. Nealson and C. R. Myers, *Am. J. Sci.* **290A**, 35 (1990).
15. This work was supported by NASA grant NAG5-6342, NSF grant OPP-9713968, and the NASA Astrobiology Institute. We thank P. Brown, and C. Bowser for donating samples for Fe isotope analysis.

16 April 1999; accepted 19 July 1999

Oxygen and Iron Isotope Studies of Magnetite Produced by Magnetotactic Bacteria

Kevin W. Mandernack,[1]* Dennis A. Bazylinski,[2] Wayne C. Shanks III,[3] Thomas D. Bullen[4]

A series of carefully controlled laboratory studies was carried out to investigate oxygen and iron isotope fractionation during the intracellular production of magnetite (Fe_3O_4) by two different species of magnetotactic bacteria at temperatures between 4° and 35°C under microaerobic and anaerobic conditions. No detectable fractionation of iron isotopes in the bacterial magnetites was observed. However, oxygen isotope measurements indicated a temperature-dependent fractionation for Fe_3O_4 and water that is consistent with that observed for Fe_3O_4 produced extracellularly by thermophilic Fe^{3+}-reducing bacteria. These results contrast with established fractionation curves estimated from either high-temperature experiments or theoretical calculations. With the fractionation curve established in this report, oxygen-18 isotope values of bacterial Fe_3O_4 may be useful in paleoenvironmental studies for determining the oxygen-18 isotope values of formation waters and for inferring paleotemperatures.

The biomineralization of Fe_3O_4 is known to occur by either biologically induced mineralization or biologically controlled mineralization (*1*). In the former, Fe_3O_4 is formed extracellularly, as a result of dissimilatory reduction of Fe^{3+} (*2*). In the latter, the Fe_3O_4 particles are produced intracellularly by magnetotactic bacteria and some higher organisms and are well-ordered crystals that exhibit narrow size distributions and species- or strain-specific morphologies (*1*). The Fe_3O_4 particles in the magnetotactic bacteria are within the single-domain size range (35 to 120 nm in length) and are usually arranged in a chain motif, providing the cell with a permanent dipole moment. This arrangement causes the cell to align along Earth's inclined geomagnetic field lines, functioning as an efficient means of locating and maintaining an optimal position in vertical chemical gradients (*3*).

Fe_3O_4-producing magnetotactic bacteria produce a number of crystal morphologies, including cubo-octahedra, elongated hexa- and octahedra, and bullet- or arrowhead-shaped forms (*1*). The presence of single-domain Fe_3O_4 crystals with these apparently unique morphologies, termed magnetofossils (*4*), as determined by electron microscopy of magnetic material separated from sediments and soils, has been used to identify the presence of magnetotactic bacteria (*5*). These apparently unique crystal forms of Fe_3O_4 have been used to distinguish a bacterial (intracellular) origin from an inorganic origin (*1, 4–9*), although not without controversy. A recent study showed that a statistical analysis of the sizes and shapes of fine-grained Fe_3O_4 crystals might prove to be a robust criterion for distinguishing between biogenic and nonbiogenic Fe_3O_4 (*10*). The presence of single-domain Fe_3O_4 with some of these morphologies has been used as evidence for the biomineralization of Fe_3O_4 by magnetotactic bacteria occurring as early as 2 billion years ago on Earth (*8*) and as partial evidence for ancient life on Mars (*11*). Stable O and Fe isotopic ratios might provide additional criteria for distinguishing between inorganically and biologically produced Fe_3O_4.

Fe_3O_4-producing magnetotactic bacteria are ubiquitous in marine and freshwater environments, where they generally inhabit the microaerobic oxic-anoxic interface (*1*). Because of their preference for environments having little or no O_2, magnetotactic bacteria may have been more widespread during Earth's ancient past, when an oxidizing aerobic atmosphere was developing (*12*). The O isotope composition [reported as $\delta^{18}O$ values (*13*)] of bacterially produced metal oxides may reflect chemical or biological origins, temperature of formation, $\delta^{18}O$ values of the formation waters, and whether molecular O_2 is incorporated during biomineralization (*14, 15*). Bacterial Mn^{4+} manganates precipitated extracellularly incorporate as much as 50% of the O from O_2, thus serving as potentially important paleo-oxygen indicators. The bacterial manganates show different $\delta^{18}O$ values from chemically produced Mn^{4+} manganates, presumably because of differences in reaction pathways or mechanisms (or both) that result in varying proportions of O derived from O_2 and H_2O being incorporated into the mineral (*15*). Because O isotopes of a variety of materials have been used to assess paleoenvironmental conditions (*16–19*), the $\delta^{18}O$ values of single-domain Fe_3O_4 particles preserved in Earth's sedimentary rock record might provide important paleoenvironmental information.

[1]Department of Chemistry and Geochemistry, Colorado School of Mines, Golden, CO 80401, USA. [2]Department of Microbiology, Iowa State University, Ames, IA 50011, USA. [3]U.S. Geological Survey, 973 Denver Federal Center, Denver, CO 80225, USA. [4]Water Resources Division, U.S. Geological Survey, MS 420, 345 Middlefield Road, Menlo Park, CA 94025, USA.

*To whom correspondence should be addressed. E-mail: kmandern@mines.edu

As a result of Fe isotope discrimination during microbial processing of Fe(III)-rich substrates, recent evidence indicates that Fe isotope variations of several per mil may result from the activity of Fe^{3+}-reducing bacteria (*20, 21*), and it has been suggested that this fractionation might be used for discerning past microbial life in ancient geological strata and perhaps in the martian meteorite ALH84001 (*22*). Theoretical calculations indicate that equilibrium Fe isotope composition differences between coexisting Fe-bearing minerals could be greater than this fractionation (*23*). Thus, we investigated the feasibility of using stable isotopic analyses ($\delta^{18}O$ and $\delta^{56}Fe$) of Fe_3O_4 produced by magnetotactic bacteria to determine whether these analyses could be used as a criterion to distinguish between the chemical and biological origins of Fe_3O_4 and whether the $\delta^{18}O$ values could serve as important paleotemperature or paleo-oxygen indicators.

We measured the $\delta^{18}O$ and $\delta^{56}Fe$ values of Fe_3O_4 produced by the following two pure cultures of obligately respiring (nonfermentative) magnetotactic bacteria grown at 28°C according to prescribed methods (*24*): *Magnetospirillum magnetotacticum* strain MS-1 (*25*), an obligate microaerophile that requires molecular O_2 to synthesize Fe_3O_4 (*12*), and strain MV-1, which grows and synthesizes Fe_3O_4 anaerobically (*26*). To determine the possible temperature effects on the $\delta^{18}O$ value of the Fe_3O_4, we also grew cells of strain MV-1 at 4° and 32°C and cells of *M. magnetotacticum* at 35°C. The bacterial Fe_3O_4 samples were purified according to tested procedures (*27*) and then analyzed for their $\delta^{18}O$ value with methods described elsewhere (*28*). In addition, using thermal ionization mass spectrometry and a double isotope spike technique (*29*), we measured the $\delta^{56}Fe$ of the Fe_3O_4 and the $FeCl_3$ and $FeSO_4$ salts provided to the bacteria to determine whether Fe isotopes are fractionated during mineral formation.

The $\delta^{56}Fe$ values of the Fe_3O_4 produced by either *M. magnetotacticum* or strain MV-1 were identical within analytical uncertainty to those of the $FeCl_3$ salt provided to both bacteria as chelated Fe^{3+} quinate in the growth medium (and to strain MV-1 as $FeSO_4$ without a chelator) (Table 1). Because of mass balance considerations, the difference in $\delta^{56}Fe$ between the accumulated product (that is, Fe_3O_4) and the starting material decreases over the course of such experiments as the $\delta^{56}Fe$ of the accumulated product progressively approaches the $\delta^{56}Fe$ of the starting material. In our experiments, the Fe salts were depleted (in mass) by amounts ranging from 45% for strain MS-1 to 87% for strain MV-1 (Table 1). By assuming that the behavior of Fe isotopes during the formation of Fe_3O_4 in these experiments can be described by a simple Rayleigh distillation process (during which the reactant becomes progressively and exponentially enriched in the less reactive isotope as the reaction approaches 100% completion), we calculated that the maximum difference in $\delta^{56}Fe$ between the Fe_3O_4 product and the Fe-salt reactant was <0.3 per mil in all cases (*30*). This amount of isotopic fractionation is minor and is essentially negligible when compared to the precision of the analytical technique.

The lack of substantial Fe isotope fractionation in intracellular Fe_3O_4 is consistent with the rate-limiting step for Fe_3O_4 formation being the passive binding of Fe ions to the external cell surface. In this case, Fe isotopic fractionation would not be likely because the limited bound Fe would be totally consumed in the crystallization process. Other nonisotopic studies have also indicated that Fe_3O_4 formation in pure cultures of *Magnetospirillum* sp. is limited by Fe availability (at dissolved Fe concentrations as low as ~20 μM) and that the availability of Fe^{2+} to the cell may be controlled by diffusive transport (*31*). Although previous work has suggested that dissimilatory Fe reduction by bacteria results in Fe isotope fractionation (*20, 21*), our results show that the absence of Fe isotope fractionation does not necessarily imply an absence of biological activity during Fe_3O_4 formation. However, because Fe isotope effects associated with microbial and chemical processes have received little investigation, interpretations at this time must be regarded with caution.

Replicates of both bacterial cultures were made under varying $\delta^{18}O$ values of the H_2O used in the growth media to determine the source of O (either H_2O or O_2) in Fe_3O_4. Because the O_2 in ambient air has a $\delta^{18}O$ value of +23.5 per mil that is distinct from that of the H_2O used in these experiments, we could determine whether molecular O_2 is incorporated into magnetotactic bacterially produced Fe_3O_4 by directly comparing the $\delta^{18}O$ values of Fe_3O_4 produced under anaerobic conditions by strain MV-1 with the $\delta^{18}O$ values of Fe_3O_4 produced under microaerobic conditions by *M. magneto-*

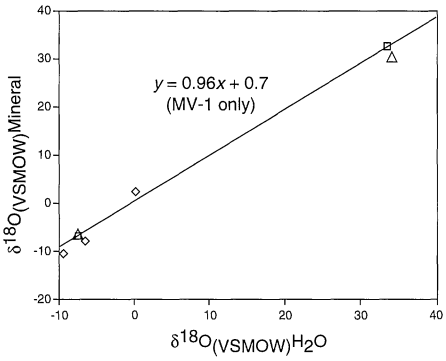

Fig. 1. The $\delta^{18}O$ value of Fe_3O_4 produced by the magnetotactic bacteria *M. magnetotacticum* strain MS-1 (triangles) and by strain MV-1 (squares), in relation to the varying $\delta^{18}O$ value of the H_2O that was added to the microbiological media used for growth during replicate cultures. *Magnetospirillum magnetotacticum* strain MS-1 is a freshwater bacterium and an obligate microaerophile, whereas MV-1 is a marine bacterium and was grown anaerobically. For each bacterium, the slope of the line is close to one, indicating that the O in Fe_3O_4 directly reflects the $\delta^{18}O$ value of the H_2O and does not incorporate molecular O_2. The results were compared to previous $\delta^{18}O$ measurements of hausmannite (Mn_3O_4) that was precipitated inorganically and by bacterial spores of a marine *Bacillus* bacterium (diamonds) [from (*15*)].

Table 1. $\delta^{18}O_{VSMOW}$ and $\delta^{56}Fe_{BIR}$ values of bacterially produced Fe_3O_4 samples. N.D., not determined; N.A., not applicable (determination of $10^3 \ln \alpha$ from these experiments is suspect because of a "memory" effect); dashes, no data available; strain MS-1, *Magnetospirillum magnetotacticum*.

Bacterial culture	Growth temperature (°C)	$\delta^{18}O$ of H_2O	$\delta^{18}O$ of Fe_3O_4	*n*	$10^3 \ln \alpha$	$\delta^{56}Fe$ of $FeCl_3$*†	$\delta^{56}Fe$ of Fe_3O_4†	*n*	[Fe]‡ (μM) Initial	[Fe]‡ (μM) Final
Strain MV-1	4	−6.9 ± 0.1	−4.3 ± 0.3	2	+2.6	−1.04	−0.97	1	28.2	3.6
Strain MV-1	28	−7.5 ± 0.1	−6.5 ± 0.05§	2	+1.0	−1.04	−1.00 ± 0.3§	3	N.D.	N.D.
Strain MV-1	28	+33.3 ± 0.6	+32.6 ± 0.1§	2	N.A.	–	N.D.	–	N.D.	N.D.
Strain MV-1	28	N.D.	N.D.	–	–	−1.55‖	−1.35	1	71.5	32.4
Strain MV-1	32	−7.6 ± 0.05	−6.7 ± 0.1	2	+0.9	–	N.D.	–	28.2	5.8
Strain MS-1	28	−7.5 ± 0.1	−6.6	1	+0.9	−1.04	−1.22 ± 0.5§	3	28.4	15.0
Strain MS-1	28	+33.8 ± 0.8	+30.3	1	N.A.	–	N.D.	–	N.D.	N.D.
Strain MS-1	35	−7.4 ± 0.03	−6.4	1	+1.0	–	N.D.	–	28.4	15.6

*$\delta^{56}Fe/^{54}Fe_{BIR}$ of $FeSO_4$ added to media in trace amounts is −1.55. †Precision at the 95% confidence level is 0.2 per mil or better. ‡As determined by the ferrozine method. §Reflects SD between replicate culture experiments. ‖Fe source is $FeSO_4$ without chelator.

tacticum. Oxygen isotopic values were similar for Fe_3O_4 produced by *M. magnetotacticum* and strain MV-1 and indicated that all of the O in the bacterial Fe_3O_4 is derived from H_2O with fractionation of ~1 per mil when grown at ~30°C (Table 1 and Fig. 1). These results are similar to previous O isotopic measurements of chemically and biologically produced hausmannite (Mn_3O_4), a Mn polymorph of Fe_3O_4 that also has cubic spinel structure and shows little isotopic fractionation (*15*). We think that the depletion in ^{18}O of the Fe_3O_4 in relation to the H_2O that was observed in both "heavy water" experiments reflects a "memory" effect from the Fe_3O_4 that was unavoidably introduced to the culture as part of the initial bacterial inoculum. This effect was larger in cultures of *M. magnetotacticum* in which cells removed less Fe from solution and produced less Fe_3O_4 than cells of strain MV-1 (Table 1).

The values of O isotope fractionation observed in our experiments are within the range of previous estimates of the fractionation between H_2O and Fe_3O_4 (Table 2) and are similar to those of Zhang *et al.* (*14*) for Fe_3O_4 produced extracellularly by a dissimilatory Fe^{3+}-reducing bacterial consortium that is thermophilic (Table 2 and Fig. 2). Previous estimates of the isotopic fractionation between inorganic Fe_3O_4 and H_2O at low temperatures may be suspect. This is due to the difficulty in chemically synthesizing Fe_3O_4 at isotopic equilibrium at temperatures <500°C. Therefore, the Fe_3O_4-H_2O fractionation curves in this temperature range have previously been largely dependent on extrapolations from experiments made at much higher temperatures (*32, 33*) or on theoretical calculations (*34*). Thus, a range of estimated fractionation values exists (Table 2).

The small O isotope fractionation that we observed in Fe_3O_4 produced by *M. magnetotacticum* and strain MV-1 at 25°C initially appeared to be consistent with O isotopic fractionation between a bacterially produced Mn^{+4} manganate and O_2 and H_2O, which were both incorporated into the mineral in equal amounts without fractionation (*15*). The lack of isotopic fractionation in this bacterially produced manganate was hypothesized to be due to rate limitation of the biomineralization process by the binding of Mn^{2+} to the cell surface. However, the $\delta^{18}O$ value of Fe_3O_4 became more enriched in ^{18}O when cells of strain MV-1 were grown at 4°C during a 2-month period, displaying a temperature-dependent fractionation (Table 1 and Fig. 2). Therefore, in the case of Fe_3O_4 produced by magnetotactic bacteria, it is possible that the lack of Fe isotopic fractionation is kinetically controlled by Fe binding to the cell surface, whereas the $\delta^{18}O$ values may reflect temperature-dependent isotopic equilibrium (kinetic isotope effects result when bacteria or other biological systems cause the isotopic value of the product to deviate from isotopic equilibrium; biological systems tend to favor the lighter isotope, but as suggested here, this is not always the case).

Zhang *et al.* (*14*) observed a temperature dependence of isotopic fractionation in Fe_3O_4 produced by a thermophilic Fe^{3+}-reducing consortium, which is consistent with the results of this study as shown by the tight correlation (combined coefficient of determination $r^2 = 0.97$) for the data of this study and of the study by Zhang *et al.* (*14*) (Fig. 2).

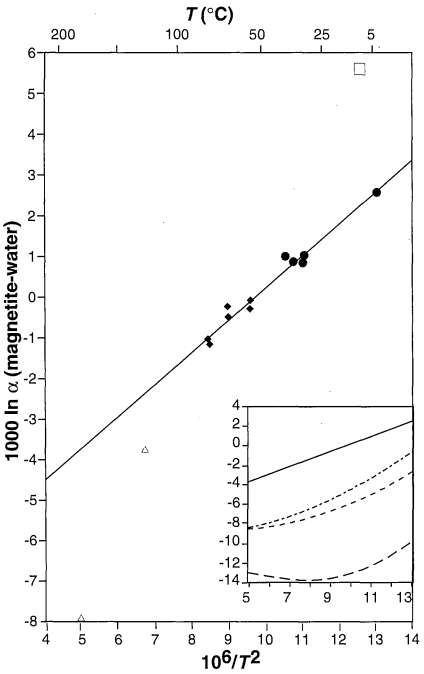

Fig. 2. Oxygen isotope fractionation (1000 ln α) between H_2O and Fe_3O_4 produced intracellularly by magnetotactic bacteria (solid circles) and extracellularly by a thermophilic dissimilatory Fe-reducing bacterial consortium (solid diamonds) (*14*) as a function of temperature. The fractionation between bacterial Fe_3O_4 and H_2O (1000 ln α) is plotted versus $10^6/T^2$ (solid line). The results of both studies form a tight correlation (combined $r^2 = 0.97$), indicating that temperature is the primary control of the variation in $\delta^{18}O$ values of bacterial Fe_3O_4 samples. The regression for this line is $1000 \ln \alpha = 7.9(10^5/T^2) - 7.64$. For comparison, we have presented the $\delta^{18}O$ results for Fe_3O_4 precipitated inorganically at temperatures of 112° and 175°C in steam pipes (open triangles) [from (*36*)] and at 9°C in the teeth of chiton, a marine mollusk (open square) [from (*35*)]. When plotted together, these results suggest a different temperature-dependent control of 1000 ln α than the bacterial Fe_3O_4 samples suggest. (**Inset**) The bacterial plot (solid line) in comparison to previous estimates of 1000 ln α for Fe_3O_4 and H_2O based on extrapolations from high-temperature experiments [short-dashed curve (*32*); long-dashed curve (*33*)] and model calculations [dotted-dashed curve (*34*)]. The curves shown are close approximates and are presented only for comparative purposes.

The combined results suggest that the temperature at which Fe_3O_4 switches from being isotopically depleted in ^{18}O with respect to H_2O to being isotopically enriched (the crossover temperature) for biogenic Fe_3O_4 and H_2O occurs at ~45°C. Bacterially produced Fe_3O_4 samples hold much promise as paleotemperature indicators at temperatures ≲100°C.

Other than the results of this study and a study by Zhang *et al.* (*14*), the only other published (to the best of our knowledge) O isotopic measurements of Fe_3O_4 that was formed at relatively low temperatures and under known conditions are of Fe_3O_4 formed in the teeth of chiton (*35*), a marine mollusk, and of Fe_3O_4 that had apparently formed inorganically at temperatures of 176° and 121°C in steam pipes (*36*) (Fig. 2). The Fe_3O_4 samples from the steam pipes are formed by Fe oxidation (*36*), and the final steps in Fe_3O_4 formation in chiton teeth reportedly involve the oxidation of Fe^{2+} (*37*). Although the reasons for Fe_3O_4 formation by the magnetotactic bacteria and Fe^{3+}-reducing bacteria are different, Fe^{3+} reduction has been detected in *M. magnetotacticum* (*38–40*), and it has been proposed that Fe^{3+} reduction is the final step of Fe_3O_4 formation by magnetotactic bacteria (*37, 40*). Thus, the common feature of Fe^{3+} reduction by magnetotactic bacteria and dissimilatory Fe^{3+}-reducing bacteria that produce Fe_3O_4 extracellularly might explain mechanistically the similarity in the temperature dependence of O isotope results in the Fe_3O_4 they produce and the contrast between the inorganically produced Fe_3O_4 and that produced biologically by chitons (Fig. 2). However, if this temperature dependence were controlled kinetically, then kinetic effects should display a time dependence that was not observed [the 28°C experiments lasted <1 week, whereas the 4°C experiment with strain MV-1 lasted for 2 months (Table 1)]. Therefore, it is possible that both bacterial systems approached isotopic equilibrium, which would explain their similarity in temperature dependence (Fig. 2). Other possible factors that might explain the differences between the bacterial data and previous measurements or estimates presented in Fig. 2 are as follows:

Table 2. Mineral-H_2O O isotope fractionation expected for Fe and Mn oxides at 25°C.

Mineral	Reference	1000 ln α
Magnetite*	This study	+1.3
Magnetite†	(*14*)	+1.3
Magnetite	(*34*)	−3.0
Magnetite	(*32*)	−4.7
Magnetite	(*36*)	+3.7
Magnetite	(*33*)	−11.3
Hematite/Goethite	(*44*)	+6.1
Hausmannite‡	(*15*)	~0

*Bacterial, intracellular. †Bacterial, extracellular. ‡At 5° to 70°C.

(i) O isotope exchange between Fe_3O_4 and H_2O is extremely slow at low temperatures, and the inorganic Fe_3O_4 samples may simply represent disequilibrium or partial isotopic equilibrium; (ii) because Fe_3O_4 contains Fe^{2+} and Fe^{3+} and because different reaction pathways for Fe_3O_4 formation may result in variations in crystal structure in which Fe^{2+} and Fe^{3+} occupy different proportions of octahedral and tetrahedral sites within the mineral, this variation in turn influences the bond energies for Fe^{2+} and Fe^{3+} and, consequently, the isotopic fractionation between Fe_3O_4 and H_2O (*41*); and (iii) bacteria exert a unique kinetic (that is, "vital") effect on the $\delta^{18}O$ values of Fe_3O_4, resulting in ^{18}O enrichment (Fig. 2), and thus show a unique temperature-dependent fractionation. For comparison, vital effects in biotically precipitated carbonates can result in shifts in both the slope and intercept on a plot of 1000 ln α versus $10^6/T^2$ ($\alpha_{mineral\text{-}H_2O}$, fractionation factor = $(\delta^{18}O_{mineral} + 1000)/(\delta^{18}O_{H_2O} + 1000)$; T, temperature in kelvin) and in some cases can result in $\delta^{18}O$ values that are higher than the equilibrium values (*42*). All of these possibilities need to be considered in future O isotope studies of Fe_3O_4.

Our results for magnetotactic bacteria, combined with results for thermophilic Fe-reducing bacteria (Fig. 2), provide a consistent correlation of 1000 ln $\alpha_{(Fe_3O_4\text{-}H_2O)}$ versus T between 4° and 70°C. Furthermore, the results are different from the established estimates of inorganic Fe_3O_4-H_2O fractionation that have been developed over the years with a variety of high-temperature experimental data (700° to 800°C), theoretical calculations, and empirical considerations (*32–34*). However, the established inorganic Fe_3O_4-H_2O fractionations may have substantial uncertainties in the low-temperature range of our experiments. Although we cannot prove equilibrium in the manner of a partial isotopic exchange experiment, we have produced pure Fe_3O_4 phases and have demonstrated a reproducible and reasonable temperature effect on O isotope fractionation. The consistency of our data with the data for thermophilic Fe-reducing bacteria indicates that we have established a reliable "bacterial fractionation curve" [1000 ln $\alpha_{(Fe_3O_4\text{-}H_2O)} = 7.9(10^5/T^2) - 7.64$] that can be used in interpreting the O isotope systematics of bacterial Fe_3O_4 samples. Therefore, if Fe_3O_4 crystals can be identified (by statistical analysis of their size and shape, for example) as having been produced by magnetotactic bacteria, then O isotopic analyses of these Fe_3O_4 particles could yield paleoenvironmental information. A mineral-pair $^{18}O/^{16}O$ thermometer (for example, calcite-magnetite) or independent knowledge of the $\delta^{18}O$ value of the waters that hosted the magnetotactic bacteria would permit the calculation of temperatures of formation.

References and Notes

1. D. A. Bazylinski and B. M. Moskowitz, *Rev. Mineral.* **35**, 181 (1997).
2. D. R. Lovley, J. F. Stolz, G. L. Nord Jr., E. J. P. Phillips, *Nature* **330**, 252 (1987).
3. R. B. Frankel, D. A. Bazylinski, M. S. Johnson, B. L. Taylor, *Biophys. J.* **73**, 994 (1997).
4. J. L. Kirschvink and S.-B. R. Chang, *Geology* **12**, 559 (1984).
5. J. F. Stolz, *J. Gen. Microbiol.* **139**, 1663 (1993).
6. J. L. Kirschvink, *Earth Planet Sci. Lett.* **59**, 388 (1982).
7. J. F. Stolz, S.-B. R. Chang, J. L. Kirschvink, *Precambrian Res.* **43**, 295 (1989).
8. S.-B. R. Chang, J. F. Stolz, J. L. Kirschvink, S. M. Awramik, *ibid.*, p. 305.
9. S.-B. R. Chang and J. L. Kirschvink, *Annu. Rev. Earth Planet. Sci.* **17**, 169 (1989).
10. B. Devouard *et al.*, *Am. Mineral.* **83**, 1387 (1998).
11. D. S. McKay *et al.*, *Science* **273**, 924 (1996).
12. R. P. Blakemore, K. A. Short, D. A. Bazylinski, C. Rosenblatt, R. B. Frankel, *Geomicrobiol. J.* **4**, 53 (1985).
13. The O isotope data are presented in terms of the Vienna standard mean ocean water (VSMOW) scale, based on standard mean ocean water having a $\delta^{18}O$ value of 0.00 per mil, whereby $\delta^{18}O_{sample}$ (in per mil) = $[(^{18}O/^{16}O_{sample})/(^{18}O/^{16}O_{VSMOW}) - 1] \times 10^3$. The Fe isotopic measurements are referenced to U.S. Geological Survey (USGS) rock standard BIR-1, an Icelandic basalt, and expressed as $\delta^{56}Fe_{sample} = [(^{56}Fe/^{54}Fe_{sample})/(^{56}Fe/^{54}Fe_{BIR}) - 1] \times 10^3$.
14. C. Zhang *et al.*, *Geochim. Cosmochim. Acta* **61**, 4621 (1997).
15. K. W. Mandernack, M. L. Fogel, B. M. Tebo, A. Usui, *ibid.* **59**, 4409 (1995).
16. L. P. Knauth and S. Epstein, *ibid.* **40**, 1095 (1976).
17. Y. Kolodny and B. Luz, in *Stable Isotope Geochemistry: A Tribute to Samuel Epstein*, vol. 3 of *Special Publications*, H. P. Taylor, J. R. O'Neil, I. R. Kaplan, Eds. (Geochemical Society, San Antonio, TX, 1991), pp. 105–119.
18. N. J. Shackleton, J. Imbrie, N. G. Pisias, J. Jose, in *The Past Three Million Years: Evolution of Climatic Variability in the North Atlantic Region*, N. J. Shackleton, R. G. West, D. Q. Bowen, Eds. (Cambridge Univ. Press, Cambridge, 1988), pp. 269–278.
19. C. J. Yapp, in *Climate Change in Continental Isotopic Records*, vol. 78 of *Geophysical Monograph Series*, P. K. Swart *et al.*, Eds. (American Geophysical Union, Washington, DC, 1993), pp. 285–294.
20. T. D. Bullen and P. M. McMahon, *Eos Trans. Am. Geophys. Union* **78**, S173 (1997).
21. B. L. Beard *et al.*, *Science* **285**, 1889 (1999).
22. R. A. Kerr, *Science* **282**, 1807 (1998).
23. V. B. Polyakov, *Geochim. Cosmochim. Acta* **61**, 4213 (1997).
24. Magnetotactic bacterial cultures used in this study included the freshwater species, *M. magnetotacticum* [American Type Culture Collection (ATCC) number 31632] (*25*), and the marine vibrio, strain MV-1 (*26*). Both were grown heterotrophically at various temperatures in 14-liter carboys; *M. magnetotacticum* was grown under microaerobic conditions (~1% O_2 in the headspace) in modified magnetic spirillum growth medium [ATCC, *Catalogue of Bacteria and Bacteriophages* (Rockville, MD, ed. 17, 1989), p. 367] containing 25 μM Fe^{3+} quinate, and strain MV-1 (*26*) was grown under anaerobic conditions in dilute artificial seawater (*43*) containing (per liter) 5.0 ml of modified Wolfe's mineral solution (*3*), 0.5 ml of vitamin solution, 0.2 ml of 0.2% aqueous resazurin, 1.5 ml of 0.5 M potassium phosphate buffer (pH 7.0), 2.5 ml of 0.01 M Fe^{3+} quinate, 0.5 g of sodium succinate·$6H_2O$, 0.5 g of Bacto-Casamino Acids (Difco Laboratories, Detroit, MI), 0.2 g of sodium acetate·$3H_2O$, 0.25 g of NH_4Cl, and 0.12 g of cysteine·HCl·H_2O under 1-atm N_2O. In cases in which chelated Fe was eliminated, the nitrilotriacetic acid was eliminated from the mineral solution, and 2.5 or 5.0 ml of 0.01 M $FeSO_4$ in 0.001 M HCl replaced the Fe^{3+} quinate solution. The final pH of this medium was adjusted to 7.1 by the addition of 0.1 M NaOH. *Magnetospirillum magnetotacticum* was grown at 28° and 35°C (maximum growth temperature), and strain MV-1 was grown at 4°, 28°, and 32°C (maximum growth temperature). Growth experiments at 28°C were performed in replicate under varying $\delta^{18}O$ values by adding ^{18}O-labeled H_2O.
25. R. P. Blakemore, D. Maratea, R. S. Wolfe, *J. Bacteriol.* **140**, 720 (1979).
26. D. A. Bazylinski, R. B. Frankel, H. W. Jannasch, *Nature* **334**, 518 (1988).
27. Cells were harvested by centrifugation (10,000*g* for 20 min at 4°C), resuspended in distilled H_2O, and lysed by three passages through a French pressure cell at 20,000 psi. Magnetosomes were magnetically separated with a gap magnet as previously described [Y. A. Gorby, T. J. Beveridge, R. P. Blakemore, *J. Bacteriol.* **170**, 834 (1988); (*43*)]. They were washed 10 times with distilled H_2O, boiled in 10% SDS for 30 min, washed 10 more times with distilled H_2O, and soaked in 5.25% sodium hypochlorite (commercial bleach) for 18 hours at 25°C. They were then washed 10 times with distilled H_2O and lyophilized. This procedure was first tested with a fine-powdered Fe_3O_4 standard using $H_2{}^{18}O$-enriched solutions of SDS and commercial bleach, which did not cause any shift in the Fe_3O_4 $\delta^{18}O$ value and efficiently removed the organic material.
28. Oxygen was extracted from bacterial Fe_3O_4 as O_2 with BrF_5 [R. N. Clayton and T. K. Mayeda, *Geochim. Cosmochim. Acta* **27**, 43 (1963)] and a laser extraction system similar to that developed by Sharp [Z. D. Sharp, *ibid.* **54**, 1353 (1990)], with CO_2 laser at a wavelength of 10.6 μm. The resulting O_2 was then converted to CO_2 for mass spectrometric analysis through reaction with a heated Pt-catalyzed graphite rod.
29. Iron isotope compositions of the Fe salts and Fe_3O_4 were determined with positive thermal ionization mass spectrometry. A double isotope spike technique was used to correct for isotope ratio shifts that can occur during Fe purification and mass spectrometry. This technique is similar to that used for ongoing research into Se isotope geochemistry at the U.S. Geological Survey in Menlo Park, CA, and is described in detail elsewhere [T. M. Johnson, T. D. Bullen, M. J. Herbel, P. T. Zawislanski, *Geochim. Cosmochim. Acta*, in press]. In brief, there are four stable Fe isotopes (^{54}Fe, ^{56}Fe, ^{57}Fe, and ^{58}Fe); our technique reports the corrected $^{56}Fe/^{54}Fe$ ratio. Before sample purification and analysis, a consistent amount of spike solution containing enriched ^{57}Fe and ^{58}Fe with a known $^{57}Fe/^{58}Fe$ ratio was added to each sample containing 1 μg of Fe. The resulting mixtures contained >90% of ^{54}Fe and ^{56}Fe from the sample and >90% of ^{57}Fe and ^{58}Fe from the spike solution. The mass ratio of sample:spike differed by <5% for all measurements listed in Table 1, thus minimizing error propagation. Samples were purified with AG1-X8 anion resin, with Teflon-distilled 6 M HCl to strip other ions and distilled H_2O to elute Fe. Ten microliters of 0.15 M H_3PO_4 were added to the eluant, the solution was dried, treated with 40 μl of H_2O_2 to eradicate organics, and dried again. The sample was loaded onto single Re filaments in a loading medium consisting of 1 μg of Al and 10 μg of colloidal silica to enhance ionization. Samples were analyzed for isotopic composition on a Finnigan MAT 261 multicollector mass spectrometer. In each case, an initial estimate of the $^{57}Fe/^{58}Fe$ ratio of the double spike was calculated on the basis of mass balance with an assumed initial composition for natural Fe (in this case, the isotope composition of Fe separated from the USGS rock standard BIR-1). The calculated $^{57}Fe/^{58}Fe$ ratio was then compared to the known value of the double spike, and an exponential mass-dependent correction factor that describes the fractionation per atomic mass unit was calculated. The measured $^{56}Fe/^{54}Fe$ ratio was then corrected according to this factor, and the process was repeated until the calculated and known $^{57}Fe/^{58}Fe$ ratios of the double spike agreed. The composition of the double spike was then subtracted from the measured ratios, providing a new estimate of the Fe isotope composition of natural Fe, and the process was repeated to convergence. The data are reported in Table 1 in standard "delta" notation as a parts per thousand (per mil) deviation

from the BIR-1 standard. All Fe isotope data listed in Table 1 are precise to 0.2 per mil or less at the 95% confidence level and represent the average of two complete procedural runs per sample.

30. The ratio of isotopic rate constants for ^{54}Fe and ^{56}Fe (k_{54}/k_{56}), referred to as the kinetic fractionation factor (kff), was calculated for the three experiments listed in Table 1 that have both Fe isotope and solution concentration data. This calculation assumes a Rayleigh distillation process controlled by a simple one-step first-order reaction. The kff was calculated according to the following equation, provided by Krouse and Tabatabai [H. R. Krouse and M. A. Tabatabai, in *Sulfur in Agriculture*, vol. 27 of *Agronomy Monograph Series*, M. A. Tabatabai, Ed. (American Society of Agronomy, Madison, WI, 1986), pp. 169–205]: $k_{54}/k_{56} = \ln(1 - F)/\ln(1 - rF)$, where F is the fraction of substrate reacted $\{1 - ([Fe]_{final}/[Fe]_{initial})\}$ and r is $(^{56}Fe/^{54}Fe_{AccumulatedProduct})/(^{56}Fe/^{54}Fe_{InitialReactant})$. Calculated values of kff are 0.99979 for strain MV-1 with chelator and 0.99971 for strain MV-1 without chelator, which correspond, respectively, to a 0.21 and 0.29 per mil instantaneous relative enrichment of ^{56}Fe in the Fe_3O_4 product. The calculated value is 1.00026 for strain MS-1 with chelator, which corresponds to a 0.26 per mil instantaneous relative depletion of ^{56}Fe in the Fe_3O_4 product. These values are only slightly greater than the maximum 2σ precision of 0.2 per mil for the Fe isotope compositions reported in Table 1, and we suggest that this level of apparent fractionation is insignificant and not convincingly resolvable with our current analytical technique. Furthermore, the Fe isotope compositions of all product-reactant pairs listed in Table 1 are essentially identical within 95% confidence limits.

31. D. Schueler and E. Baeuerlein, *Arch. Microbiol.* **166**, 301 (1996).
32. R. H. Becker and R. N. Clayton, *Geochim. Cosmochim. Acta* **40**, 1153 (1976).
33. M. W. Rowe, R. N. Clayton, T. K. Mayeda, *ibid.* **58**, 5341 (1994).
34. Y. Zheng, *ibid.* **55**, 2299 (1991).
35. J. R. O'Neil and R. N. Clayton, in *Isotopic and Cosmic Chemistry*, H. Craig, S. L. Miller, G. J. Wasserburg, Eds. (North Holland, Amsterdam, 1964), pp. 157–168.
36. P. Blattner, W. R. Braithwaite, R. B. Glover, *Isot. Geosci.* **1**, 195 (1983).
37. S. Mann, N. H. C. Sparks, V. J. Wade, in *Iron Biominerals*, R. B. Frankel and R. P. Blakemore, Eds. (Plenum, New York, 1990), pp. 21–49.
38. K. A. Short and R. P. Blakemore, *J. Bacteriol.* **167**, 729 (1986).
39. L. C. Paoletti and R. P. Blakemore, *Curr. Microbiol.* **17**, 339 (1988).
40. W. F. Guerin and R. P. Blakemore, *Appl. Environ. Microbiol.* **58**, 1102 (1992).
41. Y. Zheng, *Chem. Geol.* **121**, 309 (1995).
42. G. Wefer and W. H. Berger, *Mar. Geol.* **100**, 207 (1991).
43. D. A. Bazylinski, A. J. Garratt-Reed, R. B. Frankel, *Microsc. Res. Tech.* **27**, 389 (1994).
44. C. J. Yapp, *Chem. Geol.* **85**, 329 (1990).
45. We thank R. Frankel, M. Fogel, C. Johnson, B. Rye, M. Wahlen, Y. Gorby, and B. Hoyle for helpful discussions about this project and P. Gemery and T. Pulsipher for technical support. D.A.B. is supported by NSF grant CHE-9714101 and NASA Johnson Space Center grant NAG 9-1115.

8 April 1999; accepted 22 July 1999

Optical Measurements of Invasive Forces Exerted by Appressoria of a Plant Pathogenic Fungus

Clemens Bechinger,[1] Karl-Friedrich Giebel,[1] Martin Schnell,[1] Paul Leiderer,[1] Holger B. Deising,[3]* Martin Bastmeyer[2]*

Many plant pathogenic fungi, such as the cereal pathogen *Colletotrichum graminicola*, differentiate highly specialized infection structures called appressoria, which send a penetration peg into the underlying plant cell. Appressoria have been shown to generate enormous turgor pressure, but direct evidence for mechanical infection of plants by fungi is lacking. A microscopic method was developed that uses elastic optical waveguides to visualize and measure forces locally exerted by single appressoria. By this method, the force exerted by appressoria of *C. graminicola* was found to be about 17 micronewtons.

Plant pathogens are estimated to cause a reduction in yield of almost 20% in worldwide food and cash crops (*1*). Among these pathogens are fungi that invade plant cells to gain access to nutrients. Some fungal pathogens, such as members of the genera *Colletotrichum* or *Magnaporthe*, differentiate highly specialized infection structures called appressoria with rigid melanin-pigmented cell walls. Appressoria adhere tightly to the leaf surface of the host and develop an enormous turgor pressure by synthesizing elevated intracellular concentrations of osmotically active substances. In the causal agent of rice blast, *M. grisea*, Talbot and co-workers demonstrated that the osmoticum is glycerol, which accumulates to concentrations of more than 3 M (*2*). The plant cell is then invaded by a specialized penetration hypha that develops beneath the appressorium (*3, 4*). Previous experiments have indicated that melanization and high turgor pressure are essential for pathogenicity in *Colletotrichum* and *Magnaporthe* (*3–5*). The role of extracellular enzymes in facilitating perforation of the plant cell wall is still under debate (*4, 6*). Direct measurement of the force exerted during initial penetration, rather than indirect measurement of turgor pressure, may not only help to resolve critical aspects of host pathogen interactions, but could also facilitate the development of new antipenetrant fungicides. We introduce a technique, involving light propagation in planar waveguides, that allows optical imaging and thus direct determination of vertical forces exerted by single appressoria.

Sensing techniques based on guided optical waves have been well known for many years. The Otto and Kretschmann-Raether surface plasmon configurations are well documented as reliable methods for examining dielectric constants of thin films (*7, 8*). It is the sensitivity of such electromagnetic waves to minute modifications in the sample environment that makes optical waves useful for sensor applications. The essence of the technique is the principle of total internal reflection, which occurs when light is reflected from a surface above the critical angle Θ_c. For an interface between two different layers, $\sin \Theta_c = n_2/n_1$, where n_1 and n_2 are the optical constants of the two layers. This phenomenon is also crucial for light propagation in planar waveguides composed of a layer with high refractive index (core) sandwiched between material with lower refractive index (cladding). As a result of the interfaces, which laterally confine the electromagnetic field, only well-defined modes similar to those in a Fabry-Perot interferometer can propagate within a waveguide. The modes are characterized by a resonance condition,

$$\cos \Theta_R = m\pi/dk \qquad (m = 1, 2, 3, \ldots) \tag{1}$$

where d is the waveguide thickness, k is the wave vector inside the core, Θ_R is the angle of incidence at the cladding material, and m is the mode index.

Accordingly, if laterally resolved measurements of Θ_R are performed, Eq. 1 can be used to study the topography of a waveguide with a precision in the nanometer range. If the surface of the waveguide is deformed, for example, by the influence of vertical external forces, one obtains an image of the corresponding indentation. When the elastic constants of the waveguide are known, the local force inducing the deformation can be calculated.

To determine the local thickness of optical

[1]Faculty of Physics, [2]Faculty of Biology, University of Konstanz, Fach M626, D-78457 Konstanz, Germany. [3]Faculty of Agriculture, Phytopathology and Plant Protection, Martin-Luther-University Halle-Wittenberg, Ludwig-Wucherer-Straße 2, D-06099 Halle (Saale), Germany.

*To whom correspondence should be addressed. E-mail: martin.bastmeyer@uni-konstanz.de, deising@landw.uni-halle.de